CHARACTERIZATION OF CFRP WITH LOCKIN THERMOGRAPHY

D. Wu, R. Steegmüller, W. Karpen, and G. Busse
Institut fürKunststoffprüfung und Kunststoffkunde (IKP)
University of Stuttgart
Pfaffenwaldring 32
D-70569 Stuttgart
Germany

INTRODUCTION

Thermal waves are suited for non-contacting inspection of near-surface areas of solids [1]. The reason for this depth limitation is the strong attenuation of this modulated thermal diffusion process. The resulting depth range is frequency dependent, hence it has been pointed out very early that thermal waves allow for depth profiling by variation of modulation frequency [2, 3].

Thermal waves share with ultrasonic waves the sensitivity to boundaries. Therefore they are suited to investigate layered or laminated materials and to detect areas of thickness variations, inclusions, or disbonds. Applications are coatings and laminated polymers. Though the photothermal technique allows for remote inspection even if the sample under inspection does not have a flat surface [4, 5], thermal waves have not found major industrial application. The reason is that many relevant applications deal with material thicknesses that require very low modulation frequencies. In the conventional raster image generation mode (where one determines the thermal wave parameters at one point and then starts to measure at the next pixel) the total time for imaging is given by the number of pixels multiplied with at least the modulation period.

In reality, time required for one pixel is several cycles to achieve the stationary situation [5] and after that several cycles over which the signal is averaged. Even primitive thermal wave images may require several hours if the modulation frequency is around 1 Hz or less. It is obvious that such a slow inspection does not meet with industrial requirements. The intention of this paper is to show that lockin thermography described some time ago [6, 7] allows to detect faults in laminates within acceptable inspection time.

LOCKIN THERMOGRAPHY

The advantage of lockin thermography as compared to point-by-point photothermal raster imaging is described in Fig. 1: The basic idea of the conventional method is that one small thermal wave spot defining one pixel is inspected by one detector whose signal is analysed by one lockin-amplifier to provide local magnitude A and phase φ of the signal. Scanning requires sequential pixel inspection.

Review of Progress in Quantitative Nondestructive Evaluation, Vol. 14
Edited by D.O. Thompson and D.E. Chimenti, Plenum Press, New York, 1995

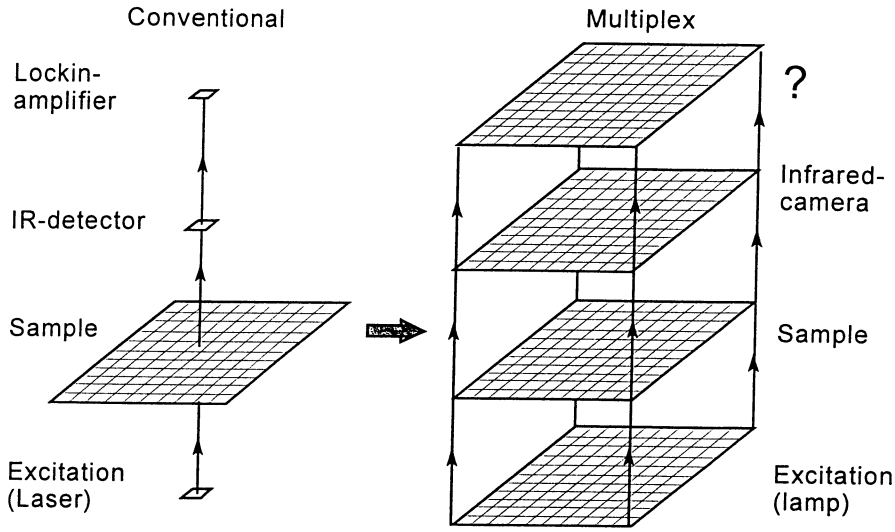

Fig. 1: Conventional and multiplex photothermal imaging.

It is obvious that it would be desirable to have many of these straight vertical lines parallel to each other. There is no problem on the source side (a lamp may generate the thermal wave everywhere) and on the detector side, since each pixel element of any thermographic camera may act as the required thermal wave detector array, even if the camera is of the scanning type. However, one cannot provide each detector element with its

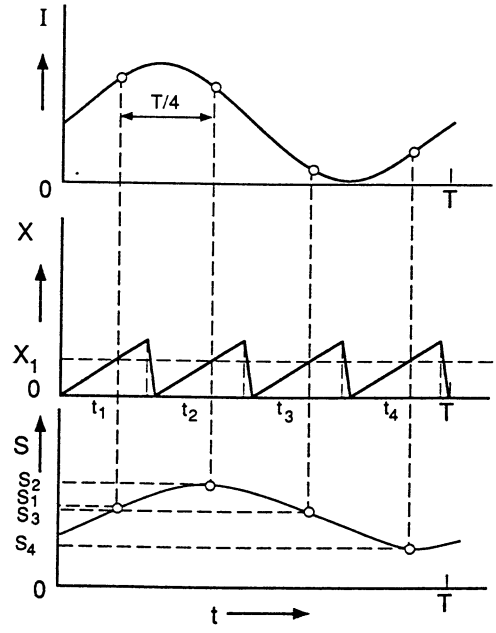

Fig. 2: Prinziple of lockin thermography (I = optical excitation, X = pixel address, S = signal reconstructed for X_1) /7/.

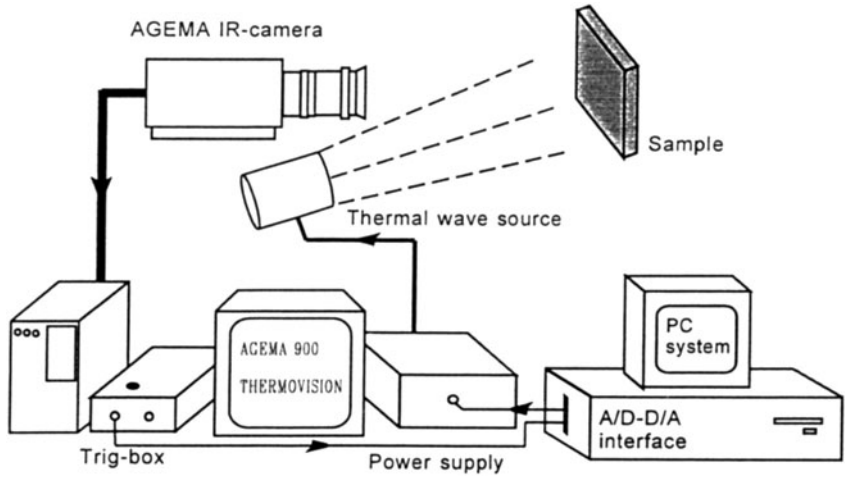

Fig. 3: Setup for Lockin thermography.

own lockin amplifier required to correlate the local temperature response to the illuminating input. It has been shown previously how thermography synchronised with modulated heat input allows for phase sensitive local detection providing an amplitude image A and a phase image φ from four primary thermographic images S_1 to S_4 obtained during one modulation cycle [7] (Fig. 2):

$$\varphi = \operatorname{arctg} \frac{S_3 - S_1}{S_4 - S_2} \tag{1}$$

$$A = \sqrt{(S_3 - S_1)^2 + (S_4 - S_2)^2} \tag{2}$$

EXPERIMENTAL MEASUREMENT

The setup that we used is displayed in Fig. 3. A commercial AGEMA 900 system is extended by a unit that synchronizes a sinusoidal modulation. Though the formalism uses the equations shown above, it should be mentioned that even at modulation frequencies as low as 0.03 Hz we use each of the thermographic images by performing a suitable averaging procedure. In fact, we also average over several modulation cycles. This way typipically around 1000 thermographic images recorded within about 2 minutes are used to calculate A and φ. Time for evaluation is between 1 and 2 minutes. The thermal wave source can be a lamp, a heat gun, or any other heat source that can be modulated in a sinusoidal way.

RESULTS

With respect to potential industrial applications our primary interest was focused on layered materials, e.g. on laminated polymers (carbon fiber reinforced plastics, CFRP).

One of the topics to be investigated is depth range in CFRP. A laminate of 2 mm thickness was provided at its rear surface with a 2 mm width rectangular slot inclined in

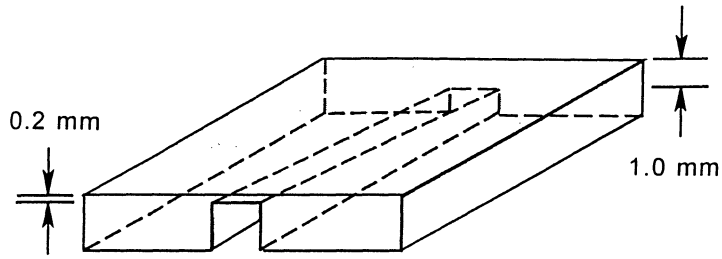

Fig. 4: Geometry of CFRP sample used for depth probing.

such a way that its distance from the front surface varied from 0.2 mm to 1.0 mm over the field of view (see Fig. 4). In Fig. 5 we show both phase and magnitude images obtained at two modulation frequencies (0.12 Hz and 0.47 Hz) The results confirm that phase has more range than magnitude and depth range is larger at lower frequencies. Since it is related to the thermal diffusion length μ given by

$$\mu = \sqrt{\frac{k}{\pi f \rho c}} \qquad (3)$$

As this slot is an artificial structure simulating the boundary of a defect (e.g. delamination), we conclude from the resulting phase angle image that depth range for defect detection is about 0.8 mm at 0.47 Hz. Based on this experimental result and equ. 3 we find that for this material frequency dependent phase angle depth range d is given by

$$d = 0.5 \text{ mm } \sqrt{Hz} \; / \sqrt{f} \qquad (4)$$

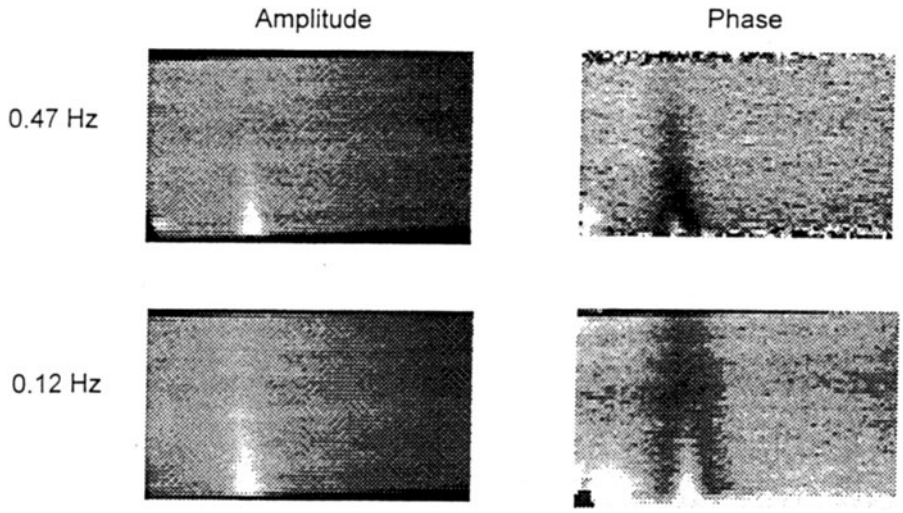

Fig. 5: Results obtained on sample of Fig. 4.

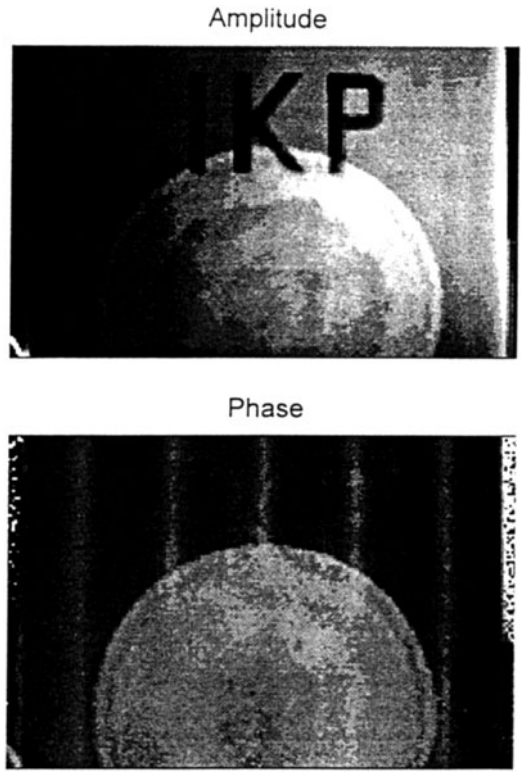

Fig. 6: Lockin thermography at 0.03 Hz on 2 mm thickness CFRP sample provided with rear surface stringers, repair pad, and surface lettering.

At the low frequency used for lockin thermography (or "multiplex thermal wave imaging") one can inspect repair pads and stringers. An example is shown in Fig. 6. The upper image was obtained using signal magnitude. Here one finds the repair area (indicated by the ring structure) and the letters "IKP" simulating optical infrared surface structure. The phase angle image (having more depth range [8]) obtained simultaneously from the same raw thermographical images reveals the stringers at the rear surface and some more repair structure while the surface structure is eliminated (except for the thermal contribution of the letters). This image shows that lockin thermography as a single-ended technique allows for monitoring the quality of repair and the adhesion of stringers.

Another topic of interest is detection of impact damage (Fig. 7). We used a CFRP laminate with surface lettering and seven impact points. Obviously the amplitude image (as well as the thermographic image) is dominated by the optical surface structure while no impact is found. The phase angle image is almost the opposite way: the weak thermal contribution of the paint is found, but the impact points are clearly visible now. The sensitivity of thermal waves to boundaries is known from previous work where point-by-point detection was used [4].

A very special boundary situation occurs in laminates when the direction of fibre orientation changes. We investigated how well one can distinguish various depth locations of such an orientation transition. The sample that we used consisted of two step-like parts

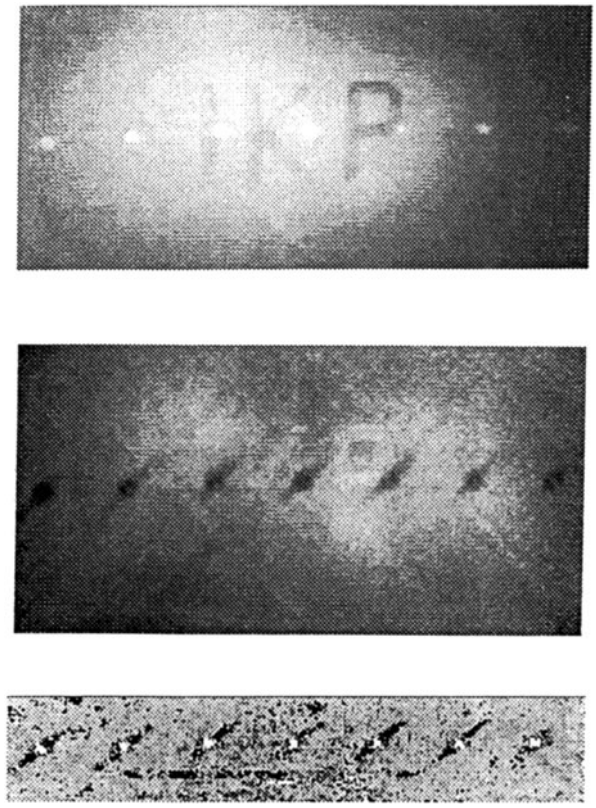

Fig. 7: CFRP sample with seven impact damage points investigated with lockin thermography (top: amplitude; middle: phase) compared to result of ultrasonic C-scan (bottom) requiring liquid coupling.

having fiber orientations perpendicular to each other, while total thickness was consistent (see Fig. 8). A laser dot shining on the surface will generate a nonspherical temperature field [9, 10]. It has been described earlier that the excentricity of the elliptical contour lines may change from the inner part to the outer part of the field if fibre orientation is not homogeneous [11-13]. The setup that we used for lockin thermographic inspection is displayed in Fig. 9 where an optical 2d-grid splits the beam of a 2 W Ar^+-laser into an array of 7 x 7 components each of which generates its own modulated laser focus. The phase angle image obtained this way is shown in Fig. 10. The elliptic pattern changes its appearence from vertical to horizontal (from left to right) with depth-dependent situations in between. Such a technique coupled to a powerful image analysis may allow for rapid monitoring of fibre orientation also in depth. So basically the technique provides information similar to microwave fibre orientation imaging presented elsewhere in this book ("Microwaves for Raster Imaging of Local Anisotropies in Polymer Materials" by L. Diener).

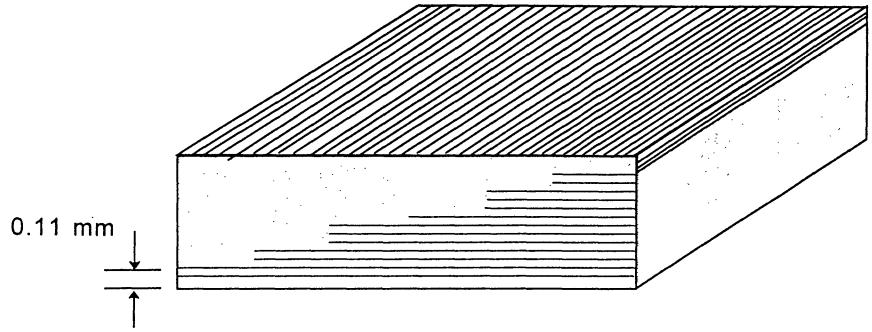

Fig. 8: CFRP sample with depth-dependent orientation of fibre orientation.

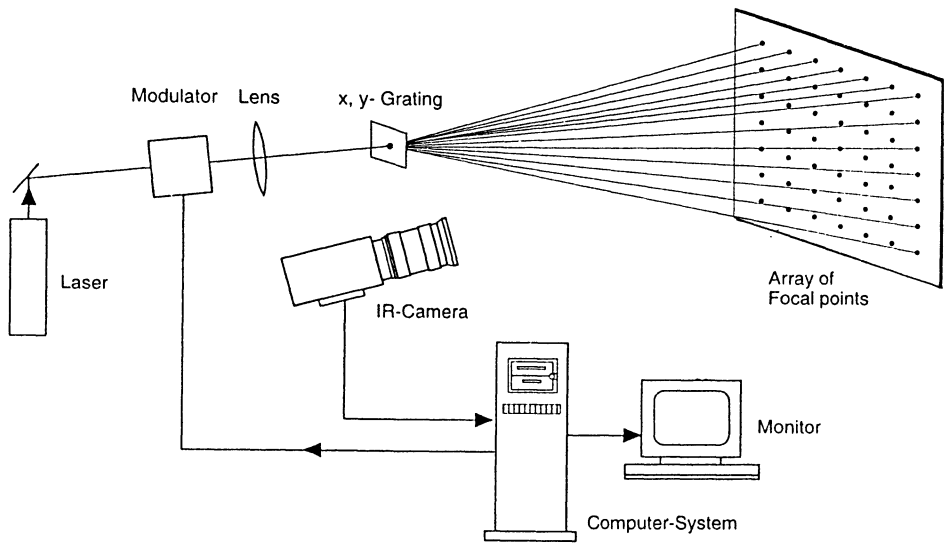

Fig. 9: Multipoint excitation for fibre orientation imaging with lockin thermography.

It should be mentioned that microwaves require low electrical conductivity (e.g. GFRP) while thermal waves work much better on CFRP than on GFRP. So obviously the two methods do not compete, each has its specific potential.

To summarize, we have shown how lockin thermography provides in a short time information on the integrity of CFRP laminates. Depth range and time required make this technique suited for industrial applications.

ACKNOWLEDGEMENT

We are grateful to AGEMA for generous support of research on lockin thermography. It is a pleasure for us to acknowledge efficient interaction with DLR (Mr. Aoki) who provided the laminates for figs. 5, 6, while depth dependent fibre orientation is investigated in EC-project Nr. BRE2-CT92-0139.

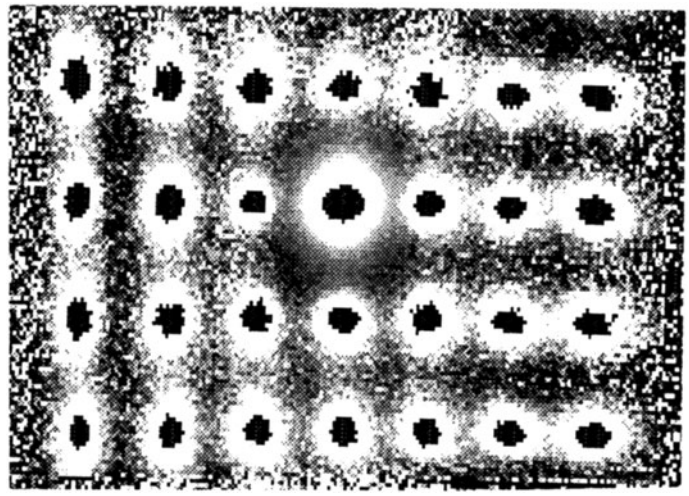

Fig. 10: Multipoint lockin thermography on sample of Fig. 8.

REFERENCES

1 A. Rosencwaig, "Photoacoustics and photoacoustic spectroscopy", John Wiley & Sons, New York, (1980)
2 A. Rosencwaig, "Photoacoustic microscopy", American Lab. 11, (1979), p. 39-49
3 G. Busse, A. Rosencwaig, "Subsurface imaging with photoacoustics", Appl. Phys. Lett. 36, (1980), p. 815-816
4 B. Rief, G. Busse, P. Eyerer, "Nondestructive testing of carbon fibre reinforced plastics (CFRP) by thermal wave radiometry, (P. Hess and J. Pelzl, eds.): Photoacoustic and Photothermal Phenomena, Springer, Heidelberg (1988), p. 447-450
5 B. Rief, "Zerstörungsfreie Charakterisierung von kohlenstoffaserverstärkten Kunststoffen mittels Wärmewellenanalyse", Diss. University Stuttgart, VDI, Düsseldorf (1988)
6 P. K. Kuo, Z. J. Feng, T. Ahmed, L. D. Favro, R. L. Thomas, J. Hartikainen, "Parallel thermal wave imaging using a vector lock-in video technique", Photoacoustic and Photothermal Phenomena, (P. Hess and J. Pelzl, eds.): Springer ser. Topics in Optical Sciences 58, Springer, Berlin (1987), p. 415-418
7 G. Busse, D. Wu, W. Karpen, "Thermal wave imaging with phase sensitive modulated thermography, J. Appl. Phys. 71, (1992), p. 3962-3965
8 G. Busse, "Optoacoustic phase angle measurement for probing a metal, Appl. Phys. Lett 35, (1979), p. 759-760
9 H. G. Kilian and M. Pietralla, "Anisotropy of thermal diffusivity of uniaxial stretched polyethylenes, Polymer, 19 (6), (1978, p. 664-672
10 M. A. Berrie, K.E. Puttick, J. G. Rider, M. Rudman, R. D. Whitehead, "Thermal probe analysis of orientation in polymers and composites, Plastics and Rubber Processing and Applications, 1 (2), (1984), p. 129-131
11 J.-C. Krapez, "Analyse de la distribution superficielle de température produite par une source concentrée de chaleur à la surface d'un matériau composite formé de couches orthotropes. Application à la mesure de l'épaisseur de ces couches", Report RT91-010-121-02, IMI, Nat. Res. Counc. Canada (1991)
12 J.-C. Krapez, P. Cielo, X. Maldague, L.A. Utracki, "Optothermal analysis of polymer composites", Polymer Composites, vol. 8 (6), (1987), p. 396-407
13 J.-C. Krapez, P. Cielo, "Transfert thermique dans un matériau formé de couches orthotropes", Eurotherm 4, Nancy 28-30 juin 1988, p. 80-83